

RESEARCH ARTICLE

Open Access



# Simulating the impact of climate change on the growth of Chinese fir plantations in Fujian province, China

Haijun Kang<sup>1,2</sup>, Brad Seely<sup>2</sup>, Guangyu Wang<sup>1,2</sup>, Yangxin Cai<sup>1</sup>, John Innes<sup>1,2</sup>, Dexiang Zheng<sup>1\*</sup>, Pingliu Chen<sup>1</sup> and Tongli Wang<sup>2</sup>

## Abstract

**Background:** Climate change represents a considerable source of uncertainty with respect to the long-term health and productivity of Chinese fir (*Cunninghamia lanceolata* (Lamb.) Hook.) plantations in southeastern China.

**Methods:** We employed the process-based, stand-level model FORECAST Climate to investigate the potential impact of four alternative climate-change scenarios on the long-term growth and development of Chinese fir plantations in Fujian province, China. The capability of the model to project seasonal patterns of productivity related to variation in temperature and moisture availability was evaluated using 11 years of 8-day composite MODIS remote sensing data.

**Results:** Simulation results suggest climate change will lead to a modest increase in long-term stemwood biomass production (6.1 to 12.1% after 30 to 60 years). The positive impact of climate change was largely attributable to both a lengthening of the growing season and an increase in nutrient-cycling rates. The increase in atmospheric CO<sub>2</sub> concentrations associated with the different emission scenarios led to an increase in water-use efficiency and a small increase in productivity. While the model predicted an overall increase in dry-season moisture stress, it did not predict increased levels of drought-related mortality.

**Conclusions:** Climate change is expected have positive impact on the growth of Chinese fir in the Fujian region of China. However, the projected increase in plantation productivity associated with climate change may not be realised if the latter also results in enhanced activity of biotic and abiotic disturbance agents.

**Keywords:** FORECAST Climate, Process simulation, Climate change, *Cunninghamia lanceolata*, Forest productivity, Nutrient cycling, MODIS

## Background

Chinese fir (*Cunninghamia lanceolata* (Lamb.) Hook.) is an evergreen conifer species and is one of the most important commercial species in China. Not only is it a valuable timber species useful for construction and furniture manufacturing (Huang 2013; Zhang et al. 2013), but it is also commonly used for pulp and biomass energy production (Nie et al. 1998; Li et al. 2013). Chinese fir has been widely planted throughout subtropical China (Yu 1997; Wu 1984), and according to the results

of the 8th National Forest Inventory, the planting area of Chinese fir is about 11.0 million ha, accounted for 15.8% of all plantations in the country (SFA 2014). In addition to its importance as a source of fibre, Chinese fir plantations also play an important role in water and soil conservation, and in climate regulation through their function as carbon sinks (Tian et al. 2002; Wang et al. 2009). Considering their large area of cultivation, and high potential for atmospheric CO<sub>2</sub> fixation (Yao et al. 2015), Chinese fir plantations represent a key component of China's greenhouse gas mitigation strategy.

There is considerable uncertainty surrounding the possible effects of climate change on the long-term health and productivity of Chinese fir plantations throughout

\* Correspondence: fjzdx123@163.com

<sup>1</sup>Forestry College, Fujian Agriculture and Forestry University, Fuzhou, Fujian 350002, China

Full list of author information is available at the end of the article

China. Deviations from historical temperature and precipitation regimes can influence a wide range of ecological processes associated with forest productivity including decomposition of dead organic matter and nutrient mineralisation rates (Gholz et al. 2000), photosynthetic rates and length of growing season (Boisvenue and Running 2006), and water stress and drought-related mortality (Allen et al. 2010). Moreover, relatively little is known about how climate change may influence the long-term growth and development of Chinese fir plantations in different parts of its range. In general, Chinese fir is adapted to warm and relatively moist climate regimes although it is also considered to be tolerant of periods of moisture stress (Wei et al. 1991). Past studies on the relationship between the growth of Chinese fir and climate factors have primarily focused on the analysis of suitable climate envelopes throughout its distribution (Wei et al. 1991; Guan 1989; Shi 1994; Wu and Hong 1984; Zhang 1995). While such studies are useful, they do not provide adequate information to inform managers how current plantations may respond to shifting climate regimes. Such information is essential to support the development of sustainable and resilient plantation management systems.

Another valuable approach to examining and monitoring the impacts of climate change is through the application of remote-sensing technologies. Satellite imagery and other remotely sensed data have been shown to be effective tools for detecting subtle long-term impacts of climate change on extensive forest areas (e.g. Keenan et al. 2014). Such data, when used in combination with ecosystem models, represent an efficient approach for projecting long-term impacts of climate change and testing model performance.

In this study we employ the process-based, forest management model FORECAST Climate to evaluate the potential impact of alternative climate change scenarios on the long-term growth and development of Chinese fir plantations in Fujian province, China. The FORECAST model (without the climate change component) has been previously applied in subtropical Chinese fir plantations to evaluate the impact of intensive short-rotation management on soil productivity (Bi et al. 2007; Xin et al. 2011). The capability of FORECAST Climate to project seasonal patterns of productivity related to variation in temperature and moisture availability was assessed using 11 years of 8-day composite MODIS remote sensing data. The broader evaluation includes an assessment of the impacts of climate change on key ecosystem processes regulating growth response.

## Methods

### Study area description

The study area was located in Shunchang County in the north central part of Fujian province (117° 29'–118° 14'

E and 26° 38'–27° 121' N). The terrain in the north and southwest is generally higher than south central areas, which contain the major rivers. Shunchang has a subtropical maritime monsoon climate, but is also influenced by a continental climate. The annual average temperature in the study area is 16.9 °C, the frost-free period lasts 305 days and the average annual rainfall is 1628 mm. With a mild and humid climate and ample sunshine and rainfall, Shunchang is suitable for the growth of Chinese fir. The specific study area includes Shuangxi Town and Yangkou Town with a total area of about 29,361 ha (Fig. 1). Spatial forest resource survey data of Shunchang County in 2007 were used as the principal data source for the analysis. Productive forests within the study area are dominated by stands of Chinese fir of ranging in age from 1 to 52 years and developed on soils with variable fertility.

### Soil description

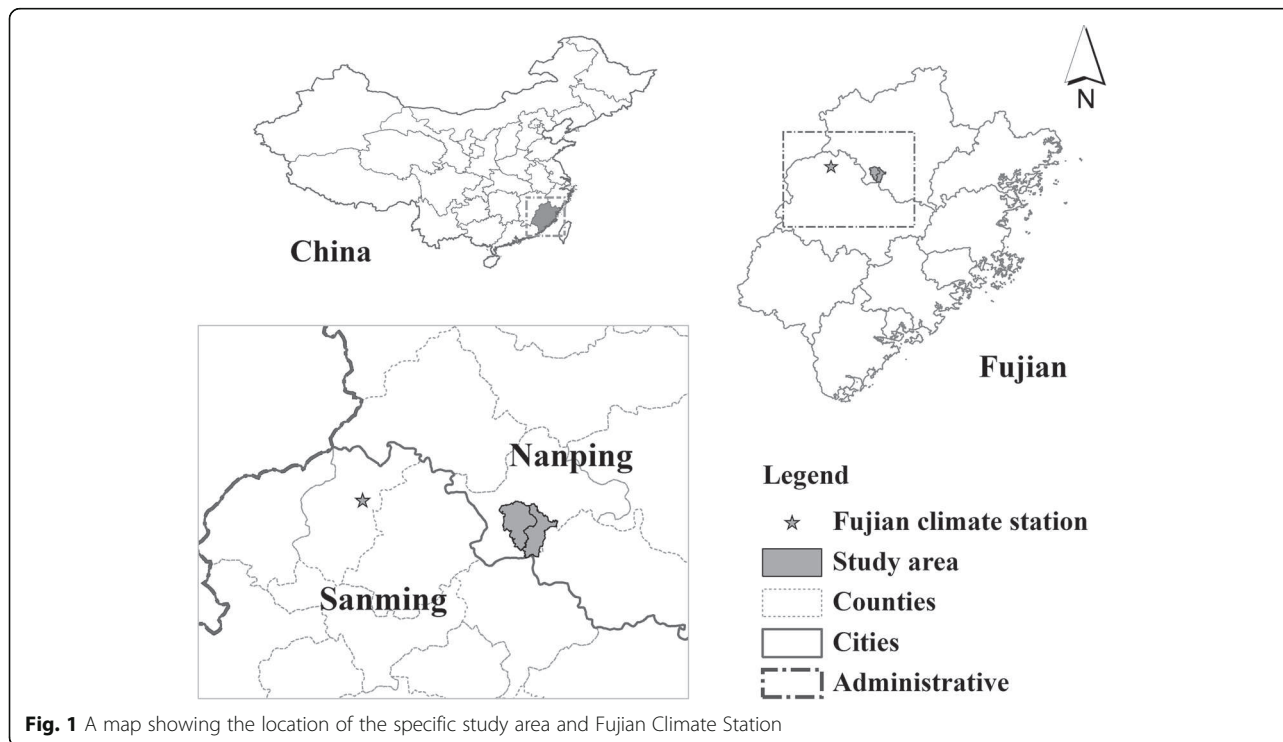
Soils within the study area are largely classified as “red earth” under the Chinese classification system (equivalent to Ultisol under USDA soil taxonomy). Soils in this region tend to be acidic, with depths greater than 1 m. The texture is mostly loam and clay, and they tend to be rich in organic matter.

### Model description

The FORECAST Climate model (Seely et al. 2015) was developed as an extension of the hybrid forest growth model FORECAST (Kimmins et al. 1999) created through the dynamic linkage of FORECAST with the stand-level hydrology model ForWaDy (Seely et al. 1997). The linked model is capable of representing the impact of climate and climate change on forest growth dynamics. Specifically, it includes detailed representations of the relationships between temperature and water availability on growth rates and as well as the effect of soil temperature and moisture contents on decomposition and nutrient cycling. The model also includes a function to represent mortality associated with severe drought events. The following sections include descriptions of the two underlying models and their linkage to form FORECAST Climate.

### The FORECAST model

The Forestry and Environmental Change Assessment Tool (FORECAST) is an ecosystem-based, stand-level growth and forest ecosystem management simulator. The model was designed to accommodate a wide variety of harvesting and silvicultural systems in order to compare and contrast their effect upon forest productivity, stand dynamics and a series of biophysical indicators of non-timber values. FORECAST employs a hybrid approach whereby local growth and yield data are used to



derive estimates of the rates of key ecosystem processes related to the productivity and resource requirements of selected species. This information is combined with data describing rates of decomposition, nutrient cycling, light competition, and other ecosystem properties to simulate forest growth under changing management conditions.

Decomposition and dead organic matter dynamics are simulated using a method in which specific biomass components are transferred, at the time of litterfall, to one of a series of independent litter types. Decomposition rates used for the main litter types represented in the model are based on the results of extensive field incubation experiments (Camiré et al. 1991; Prescott et al. 2000; Trofymow et al. 2002). Residual litter mass and associated nutrient content is transferred to active and passive humus pools at the end of the litter decomposition period (when mass remaining is approximately 15 to 20% of original litter mass). Mean residence times for active and passive humus types are typically in the range of 50 and 600 years, respectively. In FORECAST Climate, these decomposition rates are modified through the use of annual indices of temperature and moisture.

FORECAST has been widely used in Canada, Scotland, Norway, China and other countries in the world. It has been applied in variety of forest ecosystems including lodgepole pine forest (Wei et al. 2000; Wei et al. 2003), mixed aspen and white spruce forest (Seely et al. 2002; Welham et al. 2002), Scots pine forest (Blanco et al. 2006), coastal Douglas-fir forest (Blanco et al. 2007;

Morris et al. 1997), Korean larch (Sun et al. 2012), and Chinese fir plantations (Bi et al. 2007; Xin et al. 2011). The model has been used in a variety of applications and evaluated against field data for growth, yield, ecophysiological and soil variables. A detailed description of FORECAST is provided in Kimmins et al. (1999).

#### *The forest water dynamics (ForWaDy) model*

The ForWaDy model simulates the hydrologic dynamics of a forest stand on a daily time step for a given set of climatic and vegetation conditions. It has been shown to perform well for predicting the effect of forest management on evapotranspiration (Seely et al. 2006) and temporal patterns in soil moisture content under field conditions (Dordel et al. 2011; Titus et al. 2006). The model represents potential evapotranspiration (PET) using an energy balance approach based on a modified version of the Priestley-Taylor equation (Priestley and Taylor 1972). This equation has shown to be effective in predicting evapotranspiration under a wide variety of forest types and conditions (Rao et al. 2011; Stagnitti et al. 1989; Sumner and Jacobs 2005). Net shortwave solar radiation interception is used to drive the PET calculations. It is calculated for each tree and plant species from the light competition submodel built into FORECAST (Kimmins et al. 1999) and surface albedo. ForWaDy includes a representation of the vertical flow of water through canopy and soil layer compartments. Storage and movement of water in and through each soil

layer is regulated by physical properties that dictate moisture holding capacity, permanent wilting point moisture content, and infiltration rate.

Water stress is calculated for each species on a daily time step and expressed as a transpiration deficit index (TDI). The TDI is the relative difference between potential energy-limited transpiration demand and actual transpiration:

$$TDI_{i,d} = (\text{CanT}_{\text{Demand},i,d} - \text{CanT}_{\text{Actual},i,d}) / \text{CanT}_{\text{Demand},i,d} \quad (1)$$

where:

$\text{CanT}_{\text{Demand},i,d}$  = energy-driven transpiration demand for species  $i$  (mm) on day  $d$ , as a function of leaf area index (LAI), intercepted short-wave radiation, canopy albedo, and canopy resistance,

$\text{CanT}_{\text{Actual},i,d}$  = actual tree transpiration for species  $i$  (mm) on day  $d$ , as a function of  $\text{CanT}_{\text{Demand},i,d}$ , root occupancy, and available soil moisture.

A detailed description of the ForWaDy model including its general data requirements are provided in Seely et al. (2015, 1997).

#### Linking tree growth with hydrology

In the general version of the FORCAST model, forest productivity is simulated based primarily upon light and nutrient availability. FORECAST Climate was designed to incorporate explicit representations of the impact of moisture availability and temperature on forest growth processes to expand the application of the model to address potential climate change. The foundation for the expanded model was established through the creation of a dynamic linkage between the detailed representation of forest biomass growth and structure in FORECAST with the hydrological processes represented in ForWaDy (Seely et al. 2015).

#### Accounting for climate impacts on ecosystem processes

The impact of climate on tree growth and decomposition processes in FORECAST Climate is focused primarily on their relationship to temperature and water availability. These relationships are represented using curvilinear response functions, simulated on a daily time step and summarised annually. The temperature growth response functions are designed to encapsulate the physiological growth processes governing the response of trees and minor vegetation growth to mean daily temperature. The relative effect of temperature as a limiting factor on tree growth is captured annually through the sum of daily values. The positive effect of a lengthening growing season, for example, may be captured with this approach. The effect of moisture availability on plant growth rates is calculated using daily TDI values, which represent the

degree that a given tree species is able to meet its energy-driven transpiration demands. As TDI increases, plants tend to close stomata to conserve water and there is an associated reduction in photosynthetic production (McDowell et al. 2008). The model also includes a representation of the effect of increasing atmospheric  $\text{CO}_2$  concentration on water use efficiency (Seely et al. 2015).

The temperature and moisture response functions are incorporated into FORECAST Climate through their inclusion in a climate growth response index. Specifically,  $\text{GRI}_y$  is calculated for each climate year ( $y$ ) as the sum of the daily product of the temperature ( $T_{\text{Growth}}$ ) and water stress ( $S_{\text{Growth}}$ ) indices (Eqs. 2 and 3). A similar approach is used to represent the daily effect of temperature ( $T_{\text{Decomp}}$ ) and moisture content ( $M_{\text{Decomp}}$ ) on dead organic matter decomposition rates through the calculation of an annual climate decomposition response index ( $\text{DRI}_y$ , Eq. 4).

$$\text{GRI}_d = (T_{\text{Growth},d} \times S_{\text{Growth},d}) \quad (2)$$

$$\text{GRI}_y = \sum_{d=1}^{365} \text{GRI}_d \quad (3)$$

$$\text{DRI}_y = \sum_{d=1}^{365} (T_{\text{Decomp},d} \times M_{\text{Decomp},d}) \quad (4)$$

where:

$T_{\text{Growth},d}$  = The temperature growth index (range 0–1; dimensionless) on day  $d$ .

$S_{\text{Growth},d}$  = The water stress growth index (range 0–1; dimensionless) on day  $d$ .

$T_{\text{Decomp},d}$  = The temperature decomposition index (range 0–1; dimensionless) on day  $d$ .

$M_{\text{Decomp},d}$  = The moisture decomposition index (range 0–1; dimensionless) on day  $d$ .

#### FORECAST climate model calibration

The calibration of FORECAST Climate includes three steps: (1) the calibration of the FORECAST model, (2) the parameterisation of the ForWaDy model and (3) the calibration of the climate response functions in FORECAST Climate. The calibration of the base FORECAST model for Chinese fir in the Fujian region is described in Bi et al. (2007) and Xin et al. (2011) and the main calibration parameters employed in the model are provided in Additional file 1. The calibration of the climate response functions was verified using remotely sensed measures of NPP from the study area.

#### Parameterisation of the ForWaDy model

The calibration of descriptive soil variables including soil texture, coarse fragment contents and depths of soil layers and the values for key parameters describing soil water extraction and transpiration rates for Chinese fir and minor vegetation are provided in Table 1. The



original version ForWaDy has been modified to facilitate its application for climate change analysis including different CO<sub>2</sub> emissions scenarios (Seely et al. 2015). A detailed description of the representation of the effect of increasing atmospheric CO<sub>2</sub> concentrations on stomatal conductance and water use efficiency (WUE) is provided in Additional file 1. The model does not include a representation of increased atmospheric CO<sub>2</sub> concentrations on photosynthetic rates as there is little evidence to support the long-term effects of CO<sub>2</sub> fertilisation on forest productivity (See Seely et al. 2015 for a detailed discussion).

#### Calibration of climate response functions

**Growth response functions** A temperature growth response function for Chinese fir (Fig. 2a) was established based upon reported optimal temperatures from a number of studies (Zhang 1995; Wang 2006; Zhang and Xu 2002). The curve shows a sigmoidal increase in growth rate with increasing temperature up to 20 to 22 °C, representing the optimal temperature range for growth. This is followed by a declining trend as the respiration rate increases with increasing temperature (Wang 2006; Zhang and Xu 2002). Similarly, a water stress response curve was established to represent the relationship between plant growth and daily water stress (Fig. 2b). The shape of the curve is based on the model default.

**Climate impacts on decomposition** The decomposition of litter and soil organic matter in FORECAST is represented by grouping litter, created through the death of specific biomass components, into different litter types with defined mass loss rates based on litter quality and field studies (Kimmins et al. 1999). In FORECAST

Climate, these base litter decomposition rates and their associated nutrient mineralisation rates are adjusted based on mean air temperature and moisture content. The climate-influenced decomposition functions for the study area are shown in Fig. 2c, d. The shape of the temperature-decomposition response curve was based upon a Q<sub>10</sub> relationship of 2 (Zhou et al. 2008).

#### Drought-related mortality rate

FORECAST Climate includes a drought mortality function to capture the potential impacts of prolonged drought events on tree and plant mortality rates. The function simulates drought mortality using a response curve in which a 2-year running average of species-specific TDI is used as a predictor of the annual mortality rate (Fig. 3). This relationship is based upon the widely held assumption that extended periods of drought will lead to carbon starvation (Hogg et al. 2008). The shape of the curve is based on the model default derived from testing with unpublished data from several tree species in western Canada and is assumed to be relatively consistent across species.

#### Reference climate data

The FORECAST Climate model requires daily climate data to drive the simulation of climate change. Specifically, 30 years of historical climate data are suggested to provide a baseline against which any climate change scenarios can be evaluated. The Fujian climate station (see Fig. 1), near the study area, was selected for this purpose. It is located at 117.17° E and 26.9° N, with an elevation of 208 m. Daily data from 1961 to 1990 were selected to represent the 30-year reference period, including maximum temperature, minimum temperature, mean temperature and total precipitation. The average monthly

**Table 1** Parameter values in the ForWaDy submodel relevant for the simulation of plant available water, transpiration and water stress on a mesic site

| Soil variables                          | Edaphic class | Soil texture class       | Coarse fragment (%) | Mineral soil depth (cm) | Field capacity moisture content (θ)      |                                      |     |
|---|---------------|--------------------------|---------------------|-------------------------|--|--------------------------------------|-----|
|   | Mesic site    | Silt loam                | 25                  | 85                      | 0.25                                     |                                      |     |
| Soil water extraction and transpiration | Species       | Maximum LAI <sup>a</sup> | Canopy parameters   |                         | Permanent wilting point <sup>d</sup> (%) | Maximum root depth <sup>e</sup> (cm) |     |
|   |               |                          | Albedo <sup>b</sup> | Resistance <sup>c</sup> | Humus                                    | Mineral soil                         |     |
|   | Chinese fir   | 4.5                      | 0.12                | 0.3                     | 0.07                                     | 0.09                                 | 100 |
|   | Shrubs        | NA                       | 0.12                | 0.25                    | 0.08                                     | 0.1                                  | 100 |
|   | Grass         | NA                       | 0.12                | 0.2                     | 0.07                                     | 0.09                                 | 75  |

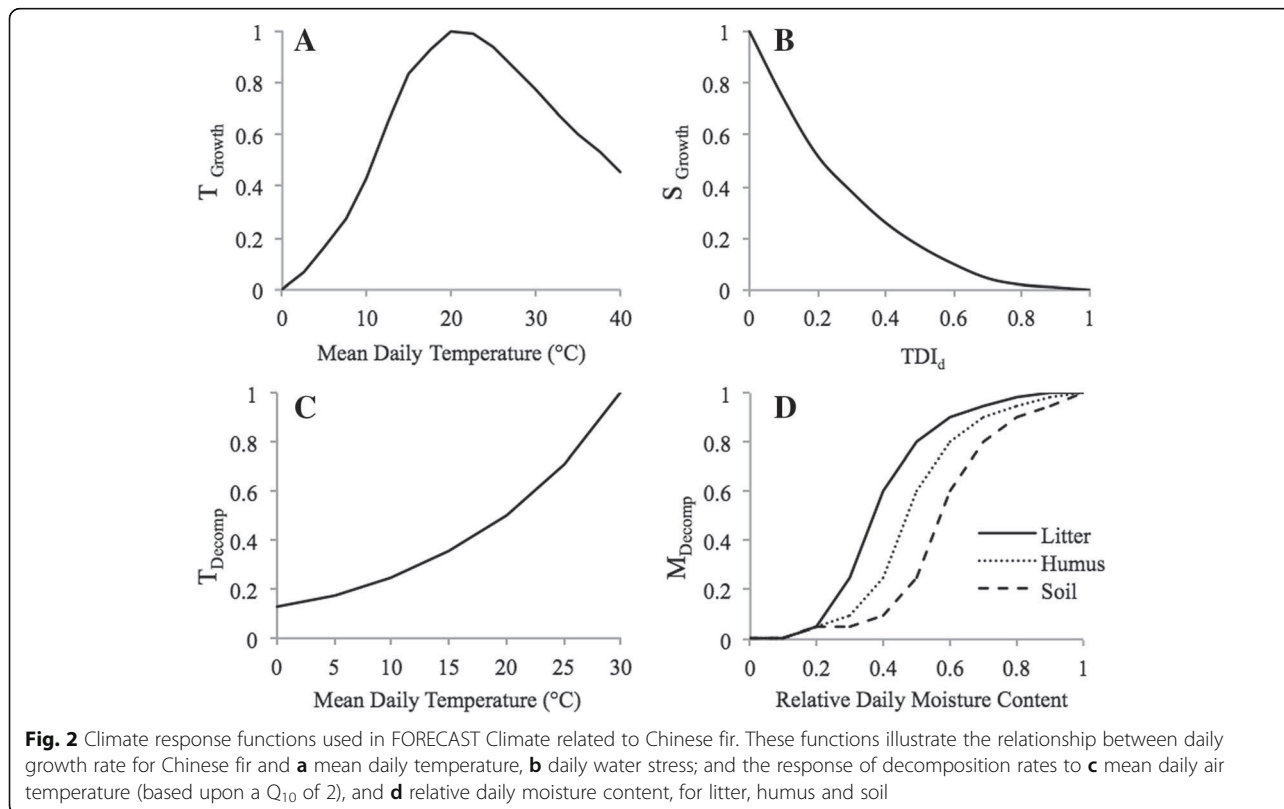
<sup>a</sup>Sets the upper limit for LAI by species. LAI is determined as a function of simulated foliage biomass. Not applicable (NA) for understorey vegetation

<sup>b</sup>Estimated values

<sup>c</sup>"Canopy resistance" represents a general measure of the resistance to water loss from foliage via stomata and cuticle. It is used to adjust the  $a$  value in the Priestley-Taylor equation to represent the amount of stomatal control on transpiration from a dry canopy based upon the relationship  $R_{Can} = 1 - (a/1.26)$  (Seely et al. 2015). An  $a$  value of 1.26 represents a freely evaporating surface, a canopy resistance value of 0.3 would reduce the  $a$  value to approximately 0.88. The value 0.3 for Chinese fir was estimated based upon the physical characteristics of its foliage and its known climate niche in comparison to other species for which values of canopy resistance have been measured (dry pine = 0.45, Douglas fir = 0.33, non-sclerophyllic broad leaves 0.13, see Seely et al. (2015))

<sup>d</sup>Refers to the volumetric moisture content at which the species can no longer extract moisture from the soil. It is related to the soil texture class

<sup>e</sup>Indicates the maximum rooting depth within the total soil profile. Estimated values



temperature and monthly total precipitation for the reference period are shown in Fig. 4.

**Calculation of climate normals**

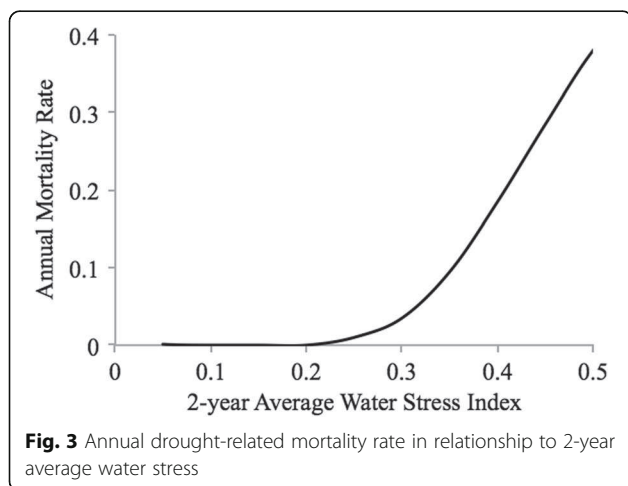
FORECAST Climate simulates the impact of climate change on growth and decomposition rates using climate normals calculated from reference climate data (Kimmins et al. 1999). Mean values for climate growth and decomposition response indices ( $GRI_{Normal}$ , and  $DRI_{Normal}$ ) were calculated by running the model in

climate calibration mode using the 30 years of daily reference climate data to drive the model without climate feedback on growth. The normal climate indices are subsequently stored for use in climate simulation runs where they are compared against simulated future climate indices to determine relative changes in baseline growth and decomposition rates.

**Application of the FORECAST climate model**

**Model validation using MODIS data**

Measurements of net photosynthesis from the Moderate Resolution Imaging Spectroradiometer (MODIS) on the NASA satellites, Terra and Aqua (Zhao et al. 2006), were used to validate the parameterised model. MODIS data were selected for evaluation as previous studies have demonstrated that MODIS estimates of GPP provide a good approximation for ground-based measures of productivity derived from eddy flux measurements in Chinese fir forests located in neighbouring Jiangxi Province (Wang et al. 2014). The data were collected during an 11-year period (2000–2010) with 8-day composite time steps. The MODIS product (MOD 17A2) provides an estimate of GPP and net photosynthesis (PSNnet) based upon direct measures of the absorption of photosynthetically active radiation (PAR) (Zhao et al. 2005).



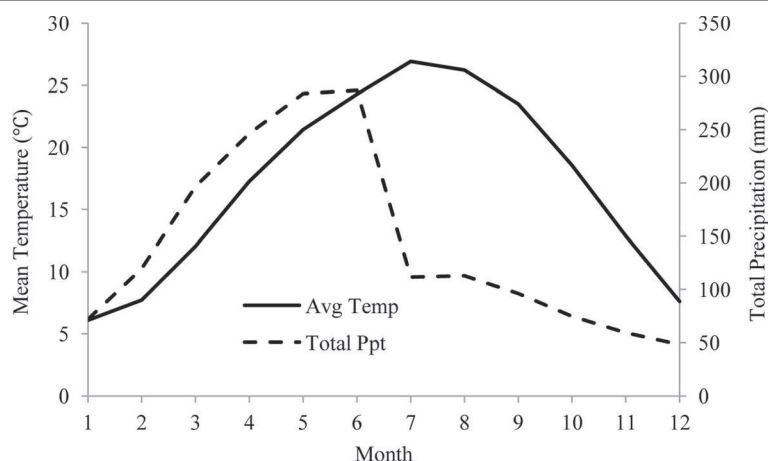


**Fig. 4** Average monthly temperature and precipitation calculated with data from the Fujian climate station, years 1961–1990

The MODIS data, available at (<http://modis.gsfc.nasa.gov/data/>), are formatted as a HDF EOS (Hierarchical Data Format – Earth Observing System) tile with a 1 km × 1 km grid in a sinusoidal projection. A total of 18 tiles with predominant Chinese fir cover were identified within the Shunchang study region (Fig. 1). A relative PSNnet value was calculated for each 8-day period for each tile and combined to produce a study-area average. Relative 8-day composite values were calculated using annual maxima for each tile. The relative values help to isolate the effects of climate on PSNnet as compared to absolute values, which are subject to differences in forest cover and other factors among tiles. Quality control data, included as part of the MOD 17A2 product (Zhao et al. 2005), were used to exclude periods for which there was excessive cloud cover or other error factors.

Daily climate data from the Fujian climate station (2000–2010) were used to drive the validation simulation of the study area with FORECAST Climate. An initial condition of a medium site quality Chinese fir plantation age 20 was established as a starting condition for the model validation exercise. For the purposes of comparison, daily output of the modelled climate growth response index ( $GRI_d$ ) was averaged for the equivalent 8-day periods used with the MODIS data.

#### **Development of climate change scenarios**

To illustrate the potential impact of climate change on long-term stand growth and development of forests in the study area, it was necessary to develop a set of alternative climate change scenarios. Two general circulation models (HadGEM2 and CNRM-CM5) included as part of the International Panel on Climate Change Fifth Assessment Report (IPCC 2013) were selected in combination with two different emission scenarios to

generate four alternative climate change projections for the study site location. The Climate models were selected to represent a general range in potential change patterns where HadGEM2 = “warm and wet” and CNRM = “cool and dry”. The two emission scenarios selected were RCP4.5 and RCP8.5, derived from the IPCC AR5 analysis (Meinshausen et al. 2011; Peters et al. 2012). Monthly outputs for the 2025, 2055 and 2085 from these models were downscaled to daily data and extrapolated for a 100-year period (2013–2112) using a direct approach linked to the daily reference climate data. In other words, the variability present in the daily reference data was projected forward in the future scenarios with the daily temperatures and precipitation amounts adjusted according to the monthly trends from the GCM models. Time periods after 2080 were assumed to have no further change other than the inherent interannual variation. Projected patterns of change in mean temperature and precipitation for the four climate change scenarios are shown in Fig. 5. Each climate data set also includes projections for annual changes in atmospheric CO<sub>2</sub> concentrations that are consistent with the associated emission scenarios.

#### **Establishment of initial conditions**

Prior to conducting a simulation run, it is necessary to establish initial soil conditions that are representative of past management activities. This is achieved by running the model in setup mode to generate an ECOSTATE file that contains values for state variables describing amounts of soil humus, decomposing litter and soil nutrient capital. We created an initial ECOSTATE file to represent a medium site (where top height = 13 m at age 20) within the study area following steps described in Bi et al. (2007).

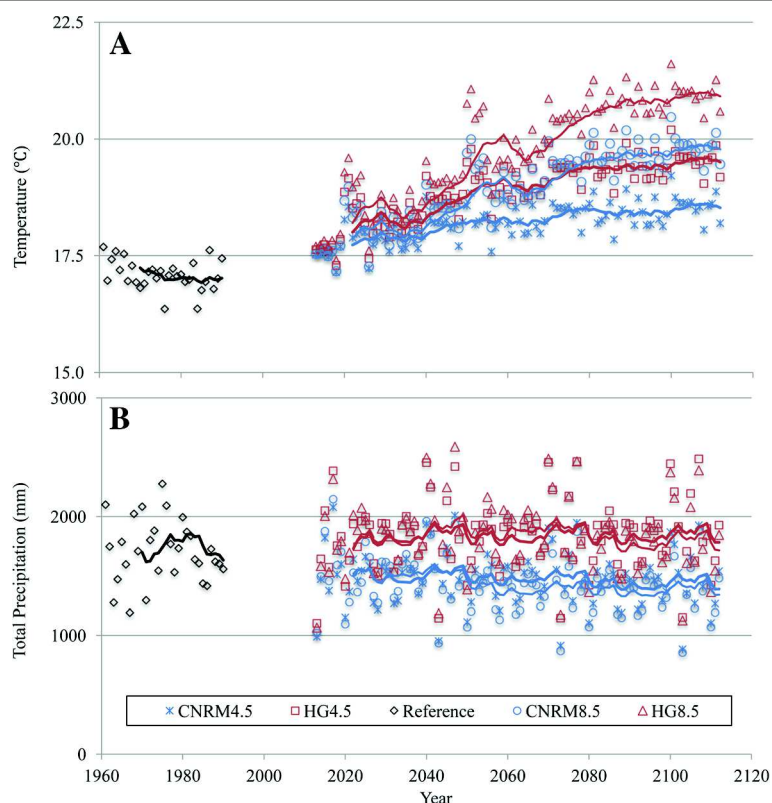


**Fig. 5** Historical reference climate data and projected pattern of change. **a, b** Mean annual air temperature and total annual precipitation for the next 100 years based on four downscaled climate change projections, respectively. Lines represent the 10-year moving average for each series

### Simulation of climate change impacts

Following the establishment of an initial ECOSTATE file, the model was used to simulate the long-term impact of climate change on the growth of Chinese fir. The four climate change scenarios described above (HG4.5, HG8.5, CNRM4.5 and CNRM8.5) and a reference climate scenario were used to drive climate simulation runs for three consecutive 30-year rotations starting in 2013. A total of five simulations were conducted.

### Sensitivity analysis

A two-part sensitivity analysis was conducted to evaluate the sensitivity of the model response to changes in atmospheric CO<sub>2</sub> concentrations and to potential changes in growing-season rainfall patterns. The impact of changing CO<sub>2</sub> concentrations was assessed by running the climate change scenarios described in the “Development of climate change scenarios” section without the corresponding changes in atmospheric CO<sub>2</sub> concentrations (atmospheric CO<sub>2</sub> was held at 396 ppm). To evaluate the impact of changes in growing season rainfall patterns, a new set of climate change scenarios were generated in which the frequency of growing season (Mar–Oct) precipitation events were reduced by 35% while maintaining the total monthly rainfall amounts.

The scenarios were created using the Statistical Downscaling Model (SDSM v5.2) developed by Wilby and Dawson (2013). These were intended to represent potential increases in rainfall intensity associated with climate warming.

## Results

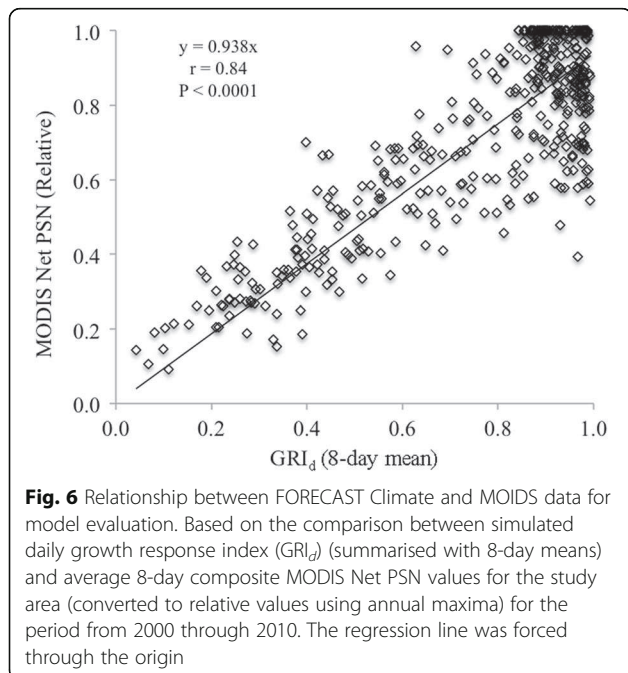
### Model evaluation against MODIS data

MODIS 8-day composite Net PSN data, averaged across 18 Chinese fir-dominated 1 km × 1 km tiles within the study area, were used to validate the capability of the model to project temporal patterns in productivity as indicated by simulated GRI<sub>d</sub>. As described above, relative values of Net PSN were calculated for each tile to better isolate the impact of climate variations on changes in productivity. There was a good correlation ( $r = 0.84$ ,  $p < 0.0001$ ) between the model and the MODIS data suggesting the model is able to represent the temporal patterns in seasonal productivity associated with temperature and moisture availability with reasonable accuracy (Fig. 6).

### Effects of climate change on tree growth

The influence of the alternative projected climate change scenarios on the simulated annual growth response



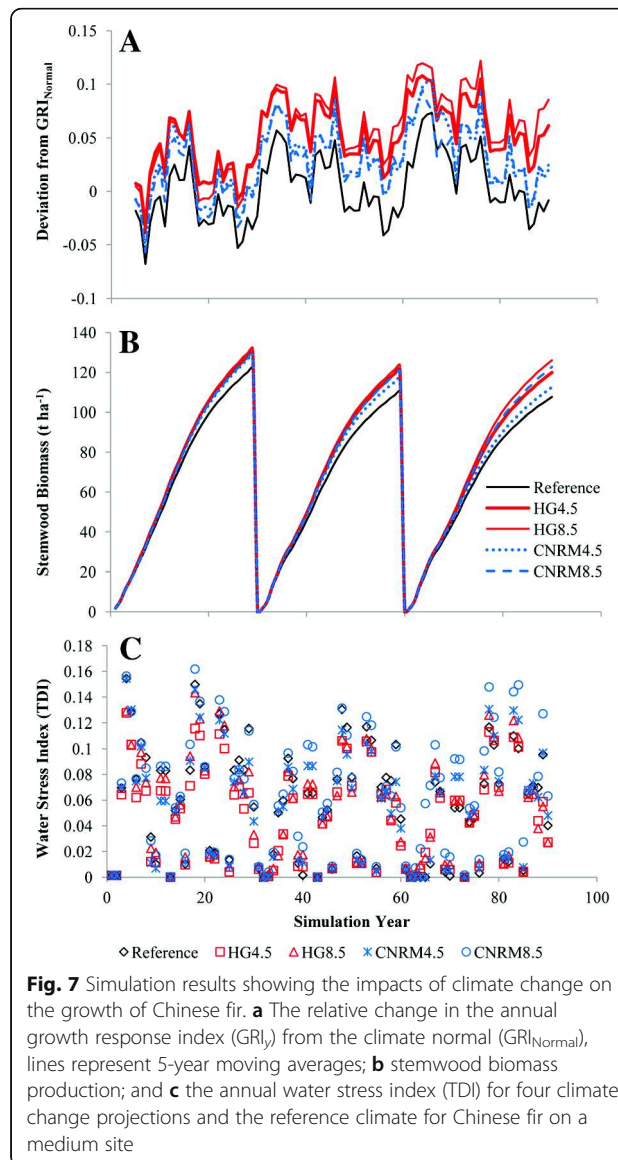


index for Chinese fir is shown in Fig. 7a. In general, the climate change scenarios showed modest increases in  $GRI_y$  relative to the reference scenario. The selection of climate model had a greater impact than the emission scenario with the HadGEM model showing the largest increase. Simulation results for stemwood biomass production followed a similar pattern (Fig. 7b) with increases in productivity of 5.4 to 8.1% by the end of the first rotation (years 1–30), 6.1 to 12.1% for the second rotation (years 31–60), and 4.5 to 17.1% for the third rotation (years 61–90).

The projected impact of the different climate change scenarios on the annual water stress index is illustrated in Fig. 7c. Water stress varies substantially year-to-year in all climate scenarios as a result of interannual variability inherent in the reference data. Scenarios based upon the CNRM-CM5 model show the highest water stress while those based upon the HadGEM2 model tend to be slightly lower than the reference climate. These results are consistent with projected rainfall trends shown in Fig. 5. Consecutive years of elevated water stress were rare in all scenarios (Fig. 7c) and, accordingly, the model projected low levels of drought-related mortality.

#### Effects of climate change on daily growth response index

To evaluate long-term trends in seasonal climate change impacts on forest growth rates, the 90-year simulations (2013–2102) were divided into three 30-year future periods (coinciding with each rotation) for each climate scenario. Model results showing the average daily growth response index of Chinese fir for the different



periods and climate scenarios are provided in Fig. 8. The daily growth response index ( $GRI_d$ ) is the product of temperature response index and water stress response index. Increases in average  $GRI_d$  were greatest during the spring and fall for all climate change scenarios. In contrast, average  $GRI_d$  tended to show modest declines in the future climate periods relative to the reference period during mid- to late summer due to higher-than-optimal temperatures and greater than normal moisture deficits. However, this negative impact was offset by a simulated lengthening of the growing season. For example, compared to reference climate, the average length of the growing season (determined as the number of calendar days in which  $T_{Growth} \geq 0.25$ ) for the period from 2073 to 2102 increased by 26 days and 34 days under the HG4.5 and HG8.5 scenarios, respectively.

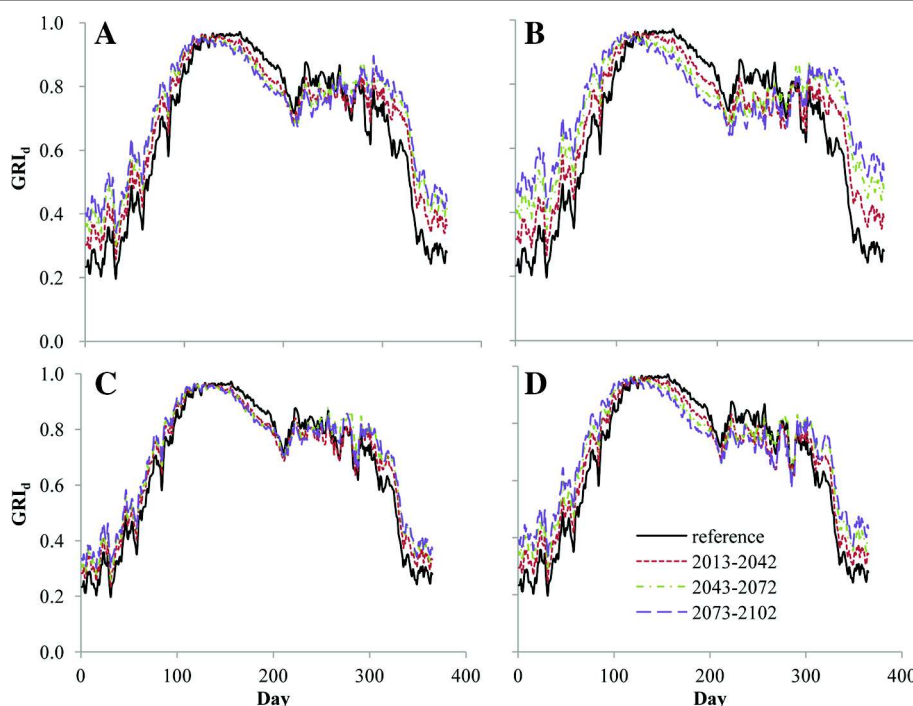


**Fig. 8** Simulation results showing the average daily growth response index. Based on three 30-year future time periods (coinciding with each rotation) relative to the reference period for the **a** HG4.5 scenario, **b** HG8.5 scenario, **c** CNRM4.5 scenario and **d** CNRM8.5 scenario

### Effects of climate change on decomposition rates and nutrient cycling

In addition to its impact on tree growth, climate change also had a positive impact on site productivity through its impact on litter decomposition rates. The litter decomposition rate index is a measure of the effect of temperature and moisture content on mass loss rates. Five-year running averages show that the litter decomposition rate increased substantially in all climate change scenarios relative to the reference climate data (Fig. 9a). The increased rates of litter decomposition led to significant increases in the rate of litter N release relative to the reference scenario (Fig. 9b), which had a positive impact on site productivity.

### Results of the sensitivity analysis

Results from the sensitivity analysis described above show that the calculation of water stress in the model is sensitive to both changes in atmospheric CO<sub>2</sub> concentration and the frequency and intensity of growing season precipitation events. Removing the effect of CO<sub>2</sub> on water use efficiency (by holding CO<sub>2</sub> constant) led to average increase of water stress of 22% above the levels observed for the original scenarios. Similarly, decreases in the frequency of growing season precipitation events led to an average increase of 24% in the mean annual water stress index (TDI) relative to the original scenarios. However, despite the increase in water stress, biomass

production at rotation only declined slightly (1 to 2%) in the sensitivity analysis runs. The impact of the increased water stress was small because although it increased, water stress was still low enough that it had only a minimal impact on growth and mortality. Detailed results from the sensitivity analysis are provided in Additional file 1.

### Discussion

#### Projections of future climate regimes

The projection of future climate regimes is invariably a source of uncertainty in modelling studies of climate change impacts on forest health and productivity. The approach taken here was to provide a range of potential patterns of change derived from the combination of two reputable climate models and two possible emission scenarios derived as part of the IPCC AR5 analysis. It should be noted that the prediction of future trends of interannual variability is extremely challenging considering most of the output from global climate models only report trends as changes in annual and monthly means and often only for particular time slices. The direct downscaling approach applied here is based upon the assumption that future patterns of interannual variability will reflect past observations. However, there is mounting evidence that this may not be the case (Wilby and Dawson 2013), particularly with respect to precipitation patterns. The sensitivity analysis conducted herein provided some

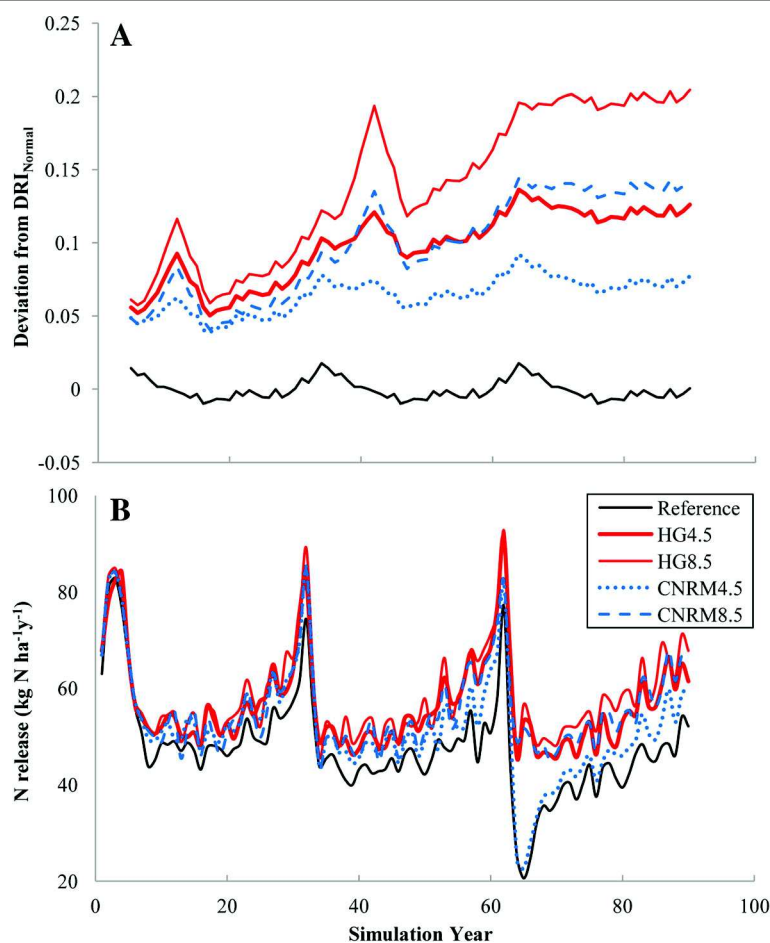


**Fig. 9** Simulation results showing the effects of climate change on decomposition rate (a) and litter nitrogen release (b). The lines in a represent 5-year moving averages

insight as to potential impact changes in the frequency of and intensity of growing season precipitation events but more work should be done in this area.

#### Effects of climate change on Chinese fir productivity

Model results suggest that Chinese fir plantations developed in the subtropical climate of Fujian province will show modest increases in productivity (6.1 to 12.1%) over the next 30 to 60 years due primarily to a lengthening of the growing season. These results are consistent with a recent study by Wang et al. (2014), who observed that productivity of Chinese fir in the Fujian region increased during a 10-year warming trend from 2000 to 2010. They suggested this pattern was linked to a prolonging of the photosynthetically active period. This conclusion is supported by a spatial-temporal climate analysis conducted by Liu et al. (2009), who reported an increase in the growing season in southeastern China of 6.9–8.7 days during the period from 1955 to 2000.

While net annual growth rates are projected to increase, FORECAST Climate predicts variably reduced

growth during the dry season as a result of increased water stress and greater-than-optimal daytime temperatures depending on the climate model selected (see Fig. 5). Predicted elevations in peak summer temperatures will exceed optimal levels causing reductions in growth during these periods, but the net positive impacts of increased growing season length were greater. Wang (2006) found that the optimal temperature and humidity required during the main period of the Chinese fir growing season were 18–20 °C and 80%, respectively. In addition, he observed that growth of Chinese fir was limited when daily temperature exceeded 28 °C and/or monthly precipitation was less than 50 mm.

Our modelling results suggest that warming associated with climate change will also benefit productivity by increasing rates of litter decomposition and associated nutrient cycling. These results are consistent with those reported by Moore et al. (1999), in a study of litter decomposition rates in Canadian forests in which litter decomposition rates were projected to increase by 4 to 7% above contemporary levels because of warming

trends expected with climate change. Evidence of the positive influence of climate enhanced decomposition and nutrient mineralisation rates on productivity has been observed by several authors. For example, Kirwan and Blum (2011) found that organic matter decomposition rates increased by about 20% per degree of warming in salt marsh experiments, which led to the enhanced productivity of marsh vegetation. Further, Melillo et al. (2011), in a 7-year soil warming study, pointed out that the plant carbon storage increased with the support of the additional inorganic nitrogen released by the warming-enhanced decay of soil organic matter.

### Projected impacts on mortality rates

While the model predicts an increase in the negative impact of dry season moisture stress on growth rates in some climate change scenarios, simulated stress levels were not high enough in consecutive years to cause increases in drought-related mortality. Several studies have observed increases in drought-related tree mortality attributed to prolonged periods of moisture stress associated with climate change (Breshears et al. 2005; Gitlin et al. 2006; van Mantgem et al. 2009; Allen et al. 2010; O'Grady et al. 2013). The reader should be reminded that the direct downscaling approach employed in the analysis presented here limits the interannual variability of future precipitation as it forces the data to follow historic patterns of variation. If interannual variation were to increase as a result of climate change, it could lead to a significant increase in drought-related mortality, which would, in turn, have a negative impact on estimates of future productivity in Chinese fir plantations. Further research is required to assess the potential of such events.

It also is important to note that FORECAST Climate does not account for the potential impacts of climate change on the activity of other disturbance agents. There is evidence that both biotic (insects and pathogens) and abiotic (fire and wind) disturbance are influenced by climate change (van Mantgem and Stephenson 2007; Mutch and Parsons 1998). O'Grady et al. (2013) pointed out that trees suffering from soil-water deficits are more susceptible to biotic disturbance agents due to significant changes in the energy and carbon balance of the plants. Thus, the predicted increases in Chinese fir plantations associated with climate change may not be realised if changes in climate regime lead to increased mortality from biotic and abiotic disturbance agents.

### Conclusions

The process-based, stand-level model FORECAST Climate was applied to examine the potential impacts of alternative climate change scenarios on the long-term growth and development of Chinese fir plantations in Fujian province. Climate change is projected to have a

modest positive impact on plantation productivity due to a gradual lengthening of the growing season and an associated increase in nutrient cycling rates. While the model predicted an increase in dry-season water stress under climate change, it did not project an increase in drought-related mortality. Moreover, the model predicted that the increases in atmospheric CO<sub>2</sub> concentrations associated with climate change would lead to increases in WUE thereby reducing the development of water stress. However, additional research should be conducted to examine the potential sensitivity of Chinese fir forests in this region to significant changes in the interannual variability in precipitation patterns associated with climate change. It is also important to note that the predicted increases in Chinese fir plantations associated with climate change may not be realised if changes in climate regime also lead to increased mortality from biotic and abiotic disturbance agents. The work presented here demonstrates the value of employing a process-based model with relatively minor calibration requirements to evaluate the potential impacts of climate change on key ecosystem processes and long-term productivity.

### Additional file

**Additional file 1:** Additional information describing the FORECAST Climate model. (DOCX 57 kb)

### Acknowledgements

This research was conducted as part of the APF Net-funded project "Adaptation of Asia-Pacific Forests to Climate Change" (project # APFNet/2010/PPF/001) founded by the Asia-Pacific Network for Sustainable Forest Management and Rehabilitation.

### Authors' contributions

BS, GW and DZ conceived and designed the study; HK and BS analysed the data; BS, JI, TW and PC contributed reagents/materials/analysis tools; HK and BS wrote the paper. All authors contributed to preparing the manuscript. All authors read and approved the final manuscript.

### Competing interests

The authors declare no conflict of interest. The founding sponsors had no role in the design of the study; in the collection, analyses, or interpretation of data; in the writing of the manuscript, and in the decision to publish the results.

### Publisher's Note

Springer Nature remains neutral with regard to jurisdictional claims in published maps and institutional affiliations.

### Author details

<sup>1</sup>Forestry College, Fujian Agriculture and Forestry University, Fuzhou, Fujian 350002, China. <sup>2</sup>Faculty of Forestry, University of British Columbia, Vancouver, BC V6T 1Z4, Canada.



Received: 23 September 2016 Accepted: 13 September 2017  
Published online: 06 October 2017

## References

- Allen, C. D., Macalady, A. K., Chenchouni, H., Bachelet, D., McDowell, N., Vennetier, M., Michel, K., Thomas, R., Andreas, B., David, D., Hogg, E. H., Gonzalez, P., Fensham, R., Zhang, Z., Castro, J., Demidova, N., Lim, J. H., Allard, G., Running, S. W., Semerci, A., & Cobb, N. (2010). A global overview of drought and heat-induced tree mortality reveals emerging climate change risks for forests. *Forest Ecology and Management*, *259*, 660–684.
- Bi, J., Blanco, J. A., Seely, B., Kimmins, J. P., Ding, Y., & Welham, C. (2007). Yield decline in Chinese-fir plantations: a simulation investigation with implications for model complexity. *Canadian Journal of Forest Research*, *37*, 1615–1630.
- Blanco, J. A., Olarieta, J. R., & Kimmins, J. P. (2006). Assessment of long-term sustainability of forest management in Scots pine forests in the Pyrenees: An ecosystem-level simulation approach. In E. Carrera, J. J. de Felipe, B. Sureda, & N. Tollin (Eds.), *International Conference on Sustainability Measurement and Modelling*. Barcelona: Centre Internacional de Mètodes Numèrics a l'Enginyeria (CIMNE).
- Blanco, J. A., Seely, B., Welham, C., Kimmins, J. P., & Seebacher, T. M. (2007). Testing the performance of a forest ecosystem model (FORECAST) against 29 years of field data in a *Pseudotsuga menziesii* plantation. *Canadian Journal of Forest Research*, *37*, 1808–1820.
- Boisvenue, C., & Running, S. W. (2006). Impacts of climate change on natural forest productivity - evidence since the middle of the 20th century. *Global Change Biology*, *12*, 862–882.
- Breshears, D. D., Cobb, N. S., Rich, P. M., Price, K. P., Allen, C. D., Balice, R. G., Romme, W. H., Kastens, J. H., Floyd, M. L., Belnap, J., Anderson, J. J., Myers, O. B., & Meyer, C. W. (2005). Regional vegetation die-off in response to global-change-type drought. *PNAS*, *102*, 15144–15148.
- Camiré, C., Côté, B., & Brulotte, S. (1991). Decomposition of roots of black alder and hybrid poplar in short-rotation plantings: Nitrogen and lignin control. *Plant and Soil*, *138*, 123–132.
- Dordel, J., Seely, B., & Simard, S. W. (2011). Relationships between simulated water stress and mortality and growth rates in underplanted *Toona ciliata* Roem. in subtropical Argentinean plantations. *Ecological Modelling*, *222*, 3226–3235.
- Gholz, H. L., Wedin, D. A., Smitherman, S. M., Harmon, M. E., & Parton, W. J. (2000). Long-term dynamics of pine and hardwood litter in contrasting environments: toward a global model of decomposition. *Global Change Biology*, *6*, 751–765.
- Gitlin, A. R., Stultz, C. M., Bowker, M. A., Stumpf, S., Paxton, K. L., Kennedy, K., Muñoz, A., Bailey, J. K., & Whitham, T. G. (2006). Mortality gradients within and among dominant plant populations as barometers of ecosystem change during extreme drought. *Conservation Biology*, *20*, 1477–1486.
- Guan, Y. (1989). A Study of the climate conditions for Chinese fir fast-growing plantations. *Chinese Journal of Agrometeorology*, *10*, 37–41.
- Hogg, E. H., Brandt, J. P., & Michaelian, M. (2008). Impacts of a regional drought on the productivity, dieback, and biomass of western Canadian aspen forests. *Canadian Journal of Forest Research*, *38*, 1373–1384.
- Huang, J. (2013). Discussion of Chinese fir planting management techniques. *Agriculture and Technology*, *33*, 77–78.
- IPCC. (2013). *Climate Change 2013: The Physical Science Basis. Contribution of Working Group I to the Fifth Assessment Report of the Intergovernmental Panel on Climate Change*. Cambridge, UK and New York, USA: Cambridge University Press.
- Keenan, T. F., Gray, J., Friedl, M. A., Toomey, M., Bohrer, G., Hollinger, D. Y., Munger, J. W., O'Keefe, J., Schmid, H. P., Wing, I. S., Yang, B., & Richardson, A. D. (2014). Net carbon uptake has increased through warming-induced changes in temperate forest phenology. *Nature Climate Change*, *4*, 598–604.
- Kimmins, J. P., Mailly, D., & Seely, B. (1999). Modelling forest ecosystem net primary production: the hybrid simulation approach used in FORECAST. *Ecological Modelling*, *122*, 195–224.
- Kirwan, M. L., & Blum, L. K. (2011). Enhanced decomposition offsets enhanced productivity and soil carbon accumulation in coastal wetlands responding to climate change. *Biogeosciences*, *8*, 987–993.
- Li, J., Chen, X., Zhu, N., Tan, Y., Yan, Y., Gao, Z., & Zhang, Y. (2013). Study on selection of main fuel-wood forest tree species in South China and combustion characteristics of wood pellets of fuel-wood trees. *Journal of Central South University of Forest & Technology*, *33*, 126–129.
- Liu, B., Henderson, M., Zhang, Y., & Xu, M. (2009). Spatiotemporal change in China's climatic growing season: 1955–2000. *Climatic Change*, *99*, 93–118.
- McDowell, N., Pockman, W. T., Allen, C. D., Breshears, D. D., Cobb, N., Kolb, T., Plaut, J., Sperry, J., West, A., Williams, D. G., & Yezzer, E. A. (2008). Mechanisms of plant survival and mortality during drought: why do some plants survive while others succumb to drought? *New Phytologist*, *178*, 719–739.
- Meinshausen, M., Smith, S. J., Calvin, K., Daniel, J. S., Kainuma, M. L. T., Lamarque, J. F., Matsumoto, K., Montzka, S. A., Raper, S. C. B., Riahi, K., Thomson, A., Velders, G. J. M., & Vuuren, D. P. P. (2011). The RCP greenhouse gas concentrations and their extensions from 1765 to 2300. *Climatic Change*, *109*, 213–241.
- Melillo, J. M., Butler, S., Johnson, J., Mohan, J., Steudler, P., Lux, H., Burrows, E., Bowles, F., Smith, R., Scott, L., Vario, C., Hill, T., Burton, A., Zhou, Y., & Tang, J. (2011). Soil warming, carbon-nitrogen interactions, and forest carbon budgets. *PNAS*, *108*, 9508–9512.
- Moore, T. R., Trofymow, J. A., Taylor, B., Prescott, C., Camiré, C., Duschene, L., Fyles, J., Kozak, L., Kranabetter, M., Morrison, I., Siltanen, M., Smith, S., Titus, B., Visser, S., Wein, R., & Zoltai, S. (1999). Litter decomposition rates in Canadian forests. *Global Change Biology*, *5*, 75–82.
- Morris, S. K., Kimmins, J. P., & Duckert, D. R. (1997). The use of soil organic matter as a criterion of the relative sustainability of forest management alternatives: a modelling approach using FORCAST. *Forest Ecology and Management*, *94*, 61–78.
- Mutch, L. S., & Parsons, D. J. (1998). Mixed conifer forest mortality and establishment before and after prescribed fire in Sequoia National Park, California. *Forest Science*, *44*, 341–355.
- Nie, S., Lin, J., Bian, L., Chen, L., & Lin, S. (1998). Evaluation of pulping properties of Chinese fir wood from plantation at different ages. *Journal of Fujian College of Forestry*, *18*, 87–91.
- O'Grady, A. P., Mitchell, P. J. M., Pinkard, E. A., & Tissue, D. T. (2013). Thirsty roots and hungry leaves: unravelling the roles of carbon and water dynamics in tree mortality. *New Phytologist*, *200*, 294–297.
- Peters, G. P., Andrew, R. M., Boden, T., Canadell, J. G., Ciais, P., Le Quééré, C., Marland, G., Raupach, M. R., & Wilson, C. (2012). The challenge to keep global warming below 2 °C. *Nature Climate Change*, *3*, 4–6.
- Prescott, C. E., Blevins, L. L., & Staley, C. L. (2000). Effects of clear-cutting on decomposition rates of litter and forest floor in forests of British Columbia. *Canadian Journal of Forest Research*, *30*, 1751–1757.
- Priestley, C. H. B., & Taylor, R. J. (1972). On the assessment of surface heat flux and evaporation using large-scale parameters. *Monthly Weather Review*, *100*, 81–92.
- Rao, L. Y., Sun, G., Ford, C. R., & Vose, J. M. (2011). Modeling potential evapotranspiration of two forested watersheds in the Southern Appalachians. *TASABE*, *54*, 2067–2078.
- Seely, B., Arp, P., & Kimmins, J. P. (1997). A forest hydrology submodel for simulating the effect of management and climate change on stand water stress. In A. Amaro & M. Tomé (Eds.), *Empirical and Process-based Models for Forest, Tree and Stand Growth Simulation* (pp. 463–477). Lisboa, Oeiras, Portugal: Edições Salamandra.
- Seely, B., Welham, C., & Elshorbagy, A. (2006). A comparison and needs assessment of hydrological models used to simulate water balance in oil sands reclamation covers. *Final Report for the Cumulative Environmental Management Association (CEMA)*. Belcarra: FORRx Consulting Inc. from <http://library.cemaonline.ca/ckan/dataset/2005-0030/resource/2ec51784-d5a2-464c-b9e3-c3aeabc781c2>. Accessed 25 Sept 2017.
- Seely, B., Welham, C., & Kimmins, J. P. (2002). Carbon sequestration in a boreal forest ecosystem: results from the ecosystem simulation model, FORECAST. *Forest Ecology and Management*, *169*, 123–135.
- Seely, B., Welham, C., & Scoullar, K. (2015). Application of a hybrid forest growth model to evaluate climate change impacts on productivity, nutrient cycling and mortality in a montane forest ecosystem. *PLoS One*, *10*(8), e0135034.
- Shi, B. (1994). Analysis of the suitable climatic conditions for Chinese fir using fuzzy comprehensive evaluation method. *Central South Forest Inventory and Planning*, *1*, 8–10.
- Stagnitti, F., Parlange, J. Y., & Rose, C. W. (1989). Hydrology of a small wet catchment. *Hydrological Processes*, *3*, 137–150.
- State Forestry Administration. (2014). General situation of forest resources in China—the 8th National Forest Inventory. Beijing.
- Sumner, D. M., & Jacobs, J. M. (2005). Utility of Penman–Monteith, Priestley–Taylor, reference evapotranspiration, and pan evaporation methods to estimate pasture evapotranspiration. *Journal of Hydrology*, *308*, 81–104.
- Sun, Z., Bi, Y., Mo, C., & Cai, T. (2012). Using an ecosystem simulation model FORECAST to evaluate the effects of forest management strategies on long-term productivity of Korean larch plantations. *Journal of Beijing Forestry University*, *34*, 1–6.
- Tian, D., Kang, W., & Wen, S. (2002). *Chinese fir plantation ecosystem ecology*. Beijing: Science Press.



- Titus, B. D., Prescott, C. E., Maynard, D. G., Mitchell, A. K., Bradley, R. L., Feller, M. C., Beese, W. J. B., Seely, B. A., Benton, R. A., Senyk, J. P., Hawkins, B. J., & Koppenaal, R. (2006). Post-harvest nitrogen cycling in clearcut and alternative silvicultural systems in a montane forest in coastal British Columbia. *The Forestry Chronicle*, *82*, 844–859.
- Trofymow, J. A., Moore, T. R., Titus, B., Prescott, C., Morrison, I., Siltanen, M., Smith, S., Fyles, J., Wein, R., Camiré, C., Duschene, L., Kozak, L., Kranabetter, M., & Visser, S. (2002). Rates of litter decomposition over 6 years in Canadian forests: influence of litter quality and climate. *Canadian Journal of Forest Research*, *32*, 789–804.
- van Mantgem, P. J., & Stephenson, N. L. (2007). Apparent climatically induced increase of tree mortality rates in a temperate forest. *Ecology Letters*, *10*, 909–916.
- van Mantgem, P. J., Stephenson, N. L., Byrne, J. C., Daniels, L. D., Franklin, J. F., Fulé, P. Z., Harmon, M. E., Larson, A. J., Smith, J. M., Taylor, A. H., & Veblen, T. T. (2009). Widespread increase of tree mortality rates in the western United States. *Science*, *323*, 521–524.
- Wang, B., Ma, X., Guo, H., Wang, Y., & Leng, L. (2009). Evaluation of the Chinese fir forest ecosystem services value. *Scientia Silvae Sinicae*, *45*, 124–130.
- Wang, C. (2006). Analysis on the relationships between the phenology and growth process of Chinese fir and climate factors in Henan Province. *XIANDAINONGYE KEJI*, *9*(5–6), 16.
- Wang, L., Zhang, Y., Berninger, F., & Duan, B. (2014). Net primary production of Chinese fir plantation ecosystems and its relationship to climate. *Biogeosciences*, *11*, 5595–5606.
- Wei, G., Deng, Y., Xiao, T., Zhong, L., Liu, J., & Tong, S. (1991). Analysis on the annual growth pulse of young Chinese fir stand and its relevant climate factors. *Journal of Sichuan Forestry Science and Technology*, *12*, 15–22.
- Wei, X., Kimmins, J. P., & Zhou, G. (2003). Disturbances and the sustainability of long-term site productivity in lodgepole pine forests in the central interior of British Columbia—an ecosystem modeling approach. *Ecological Modelling*, *164*, 239–256.
- Wei, X., Liu, W., Waterhouse, J., & Armleder, M. (2000). Simulations on impacts of different management strategies on long-term site productivity in lodgepole pine forests of the central interior of British Columbia. *Forest Ecology and Management*, *133*, 217–229.
- Welham, C., Seely, B., & Kimmins, J. P. (2002). The utility of the two-pass harvesting system: an analysis using the ecosystem simulation model FORECAST. *Canadian Journal of Forest Research*, *32*, 1071–1079.
- Wilby, R. L., & Dawson, C. W. (2013). The statistical downscaling model: insights from one decade of application. *International Journal of Climatology*, *33*, 1707–1719.
- Wu, J., & Hong, W. (1984). A study of the climatology for Chinese fir. *Meteorological Science and Technology*, *1*, 74–75.
- Wu, Z. (1984). *Chinese-fir*. Beijing: China Forestry Publishing House.
- Xin, Z., Jiang, H., Jie, C., Wei, X., Juan, B., & Zhou, G. (2011). Simulated nitrogen dynamics for a *Cunninghamia lanceolata* plantation with selected rotation ages. *Journal of Zhejiang A&F University*, *28*, 855–862.
- Yao, L., Kang, W., Zhao, Z., & He, J. (2015). Carbon fixed characteristics of plant of Chinese fir (*Cunninghamia lanceolata*) plantation at different growth stages in Huitong. *Acta Ecologica Sinica*, *35*, 1–16.
- Yu, X. (1997). *Silviculture of Chinese-fir*. Fuzhou: Science and Technology Press of Fujian.
- Zhang, X., Duan, A., & Zhang, J. (2013). Tree biomass estimation of Chinese fir based on Bayesian method. *PLoS One*, *8*, 1–7.
- Zhang, X., & Xu, D. (2002). Effects of temperature on the photosynthetic physio-ecology of 18-year-old Chinese fir. *Scientia Silvae Sinicae*, *38*, 27–33.
- Zhang, Y. (1995). A study of the effects of climatic fluctuation on Chinese fir and bamboo ecological environment in subtropical regions in China. *Quarterly Journal of Applied Meteorology*, *6*, 75–82.
- Zhao, M., Heinsch, F. A., Nemani, R. R., & Running, S. W. (2005). Improvements of the MODIS terrestrial gross and net primary production global data set. *Remote Sensing of Environment*, *95*, 164–176.
- Zhao, M., Running, S. W., & Nemani, R. R. (2006). Sensitivity of Moderate Resolution Imaging Spectroradiometer (MODIS) terrestrial primary production to the accuracy of meteorological reanalyses. *Journal of Geophysical Research*, *111*, 2005–2012.
- Zhou, G., Guan, L., Wei, X., Tang, X., Liu, S., Liu, J., Zhang, D., & Yan, J. (2008). Factors influencing leaf litter decomposition: an intersite decomposition experiment across China. *Plant and Soil*, *311*, 61–72.

**Submit your manuscript to a SpringerOpen® journal and benefit from:**

- Convenient online submission
- Rigorous peer review
- Open access: articles freely available online
- High visibility within the field
- Retaining the copyright to your article

Submit your next manuscript at ► [springeropen.com](http://springeropen.com)

## **Additional file 1**

### **Additional Information Describing the FORECAST Climate Model**

Haijun Kang<sup>1,2</sup>, Brad Seely<sup>2</sup>, Guangyu Wang<sup>1,2</sup>, Yangxin Cai<sup>1</sup>, John Innes<sup>1,2</sup>, Dexiang Zheng<sup>1\*</sup>, Pingliu Chen<sup>1</sup> and Tongli Wang<sup>2</sup>

<sup>1</sup> Forestry College, Fujian Agriculture and Forestry University, Fuzhou, Fujian, 350002, China

<sup>2</sup> Faculty of Forestry, University of British Columbia, Vancouver, British Columbia, V6T 1Z4, Canada

\* Corresponding author : Dexiang Zheng

E-mail: fjzdx123@163.com

## **1 FORECAST Model Calibration for Chinese fir**

The calibration of FORECAST includes two stages (Blanco et al., 2007): 1) data assembly, input, and validation; 2) establishing the ecosystem condition for the beginning of a simulation run (by simulating the known or assumed history of the site). Calibration input data for FORECAST were principally derived from mensuration datasets from a range of Chinese fir forests located within southeastern China and varying in age and nutritional quality (Wei and Blanco, 2014). Additional data were obtained from relevant literature, including research reports from Fujian, Hunan, Jiangxi, Guangxi and other climatically similar regions (Xin et al., 2011). The main calibration parameters employed in the model are provided in Tables S1, S2 and S3. In the second stage, FORECAST was run in set-up mode to generate initial site conditions (forest floor and soil organic matter contents that were consistent with observed site conditions).

Table S1. Data defining the growth of Chinese fir used in FORECAST

| Parameter  | Unit                   | Stand age (y) |      |      |      |       |       |       |       |       |       |
|--|------------------------|---------------|------|------|------|-------|-------|-------|-------|-------|-------|
|  |                        | 1             | 3    | 5    | 10   | 15    | 21    | 31    | 43    | 50    | 100   |
| Stemwood biomass accumulation (poor site)          | t ha <sup>-1</sup>     | 0.1           | 0.9  | 10.6 | 28.0 | 49.2  | 68.5  | 83.0  | 90.0  | 94.5  | 97.0  |
| Stemwood biomass accumulation (medium site)        | t ha <sup>-1</sup>     | 0.3           | 1.7  | 15.8 | 41.4 | 84.2  | 126.9 | 159.0 | 175.0 | 183.0 | 186.0 |
| Stemwood biomass accumulation (good site)          | t ha <sup>-1</sup>     | 0.5           | 4.7  | 27.4 | 70.0 | 128.0 | 184.0 | 234.0 | 262.0 | 273.0 | 278.0 |
| Bark biomass accumulation (poor site)              | t ha <sup>-1</sup>     | 0.0           | 0.0  | 0.6  | 3.5  | 5.8   | 10.0  | 13.8  | 15.9  | 17.4  | 18.0  |
| Bark biomass accumulation (medium site)            | t ha <sup>-1</sup>     | 0.0           | 0.1  | 1.6  | 5.5  | 10.3  | 16.5  | 23.5  | 26.5  | 29.0  | 30.5  |
| Bark biomass accumulation (good site)              | t ha <sup>-1</sup>     | 0.0           | 0.2  | 1.4  | 7.7  | 13.6  | 24.9  | 35.3  | 40.7  | 44.0  | 46.0  |
| Branch biomass accumulation (poor site)            | t ha <sup>-1</sup>     | 0.0           | 0.2  | 1.7  | 4.2  | 6.2   | 7.4   | 8.1   | 8.3   | 8.1   | 7.9   |
| Branch biomass accumulation (medium site)          | t ha <sup>-1</sup>     | 0.0           | 0.3  | 2.2  | 5.5  | 7.8   | 9.5   | 11.3  | 12.2  | 12.6  | 12.9  |
| Branch biomass accumulation (good site)            | t ha <sup>-1</sup>     | 0.0           | 0.6  | 3.7  | 7.0  | 9.8   | 11.9  | 14.7  | 16.6  | 17.5  | 17.9  |
| Foliage biomass accumulation (poor site)           | t ha <sup>-1</sup>     | 0.1           | 0.3  | 2.8  | 6.9  | 7.4   | 7.1   | 6.5   | 5.5   | 4.7   | 3.8   |
| Foliage biomass accumulation (medium site)         | t ha <sup>-1</sup>     | 0.2           | 0.6  | 4.1  | 10.5 | 11.0  | 10.7  | 10.3  | 8.8   | 7.4   | 6.0   |
| Foliage biomass accumulation (good site)           | t ha <sup>-1</sup>     | 0.3           | 0.9  | 6.5  | 16.5 | 16.2  | 15.6  | 14.3  | 12.2  | 10.3  | 8.3   |
| Large roots biomass accumulation (poor site)       | t ha <sup>-1</sup>     | 0.0           | 0.0  | 0.5  | 6.4  | 12.3  | 17.6  | 21.2  | 22.2  | 22.8  | 19.6  |
| Large roots biomass accumulation (medium site)     | t ha <sup>-1</sup>     | 0.0           | 0.0  | 2.2  | 11.1 | 22.7  | 34.0  | 42.0  | 44.7  | 45.9  | 39.8  |
| Large roots biomass accumulation (good site)       | t ha <sup>-1</sup>     | 0.0           | 0.1  | 5.7  | 20.2 | 35.5  | 51.0  | 63.6  | 68.8  | 70.4  | 61.4  |
| Small roots biomass accumulation (poor site)       | t ha <sup>-1</sup>     | 0.1           | 0.2  | 1.9  | 4.7  | 5.0   | 4.8   | 4.4   | 3.7   | 3.2   | 2.5   |
| Small roots biomass accumulation (medium site)     | t ha <sup>-1</sup>     | 0.1           | 0.3  | 2.1  | 5.3  | 5.5   | 5.4   | 5.2   | 4.4   | 3.7   | 3.0   |
| Small roots biomass accumulation (good site)       | t ha <sup>-1</sup>     | 0.1           | 0.3  | 2.4  | 6.0  | 5.9   | 5.7   | 5.2   | 4.4   | 3.8   | 3.0   |
| Average top height of dominant trees (poor site)   | m                      | 0.4           | 1.0  | 2.5  | 5.8  | 9.3   | 12.6  | 15.4  | 16.4  | 17.0  | 18.6  |
| Average top height of dominant trees (medium site) | m                      | 0.5           | 1.8  | 3.6  | 8.4  | 12.6  | 15.5  | 17.5  | 19.2  | 20.6  | 23.4  |
| Average top height of dominant trees (good site)   | m                      | 0.7           | 2.7  | 5.1  | 11.6 | 17.4  | 20.4  | 22.1  | 24.0  | 25.8  | 28.6  |
| Stand density (poor site)                          | stems ha <sup>-1</sup> | 3000          | 2850 | 2800 | 2700 | 2500  | 2350  | 2250  | 2150  | 2050  | 1400  |
| Stand density (medium site)                        | stems ha <sup>-1</sup> | 3000          | 2850 | 2800 | 2600 | 2300  | 2100  | 2000  | 1900  | 1820  | 1260  |
| Stand density (good site)                          | stems ha <sup>-1</sup> | 3000          | 2850 | 2800 | 2500 | 2100  | 1900  | 1750  | 1620  | 1550  | 1050  |

Table S2. FORECAST calibration parameters related to the simulation of litter decomposition and nutrient cycling for Chinese fir (after Wei and Blanco, 2014).

| Parameter   | Unit                 | Rich site   | Medium site    | Poor site      |
|---|----------------------|---|----------------|----------------|
| <b><i>Chinese fir parameters</i></b>                    |                      |   |                |                |
| Nitrogen concentration in stem sapwood/heartwood        | %                    | 0.14/0.03   | 0.13/0.03      | 0.12/0.03      |
| Nitrogen concentration in bark live/dead                | %                    | 0.44/0.27   | 0.40/0.25      | 0.38/0.24      |
| Nitrogen concentration in branches live/dead            | %                    | 0.67/0.52   | 0.61/0.50      | 0.55/0.47      |
| Nitrogen concentration in foliage young/old/dead        | %                    | 1.53/1.36/1.13  | 1.37/1.24/1.03 | 1.21/1.11/0.93 |
| Nitrogen concentration in large root sapwood/heartwood  | %                    | 0.37/0.06   | 0.35/0.06      | 0.34/0.05      |
| Nitrogen concentration in medium root sapwood/heartwood | %                    | 0.43/0.07   | 0.39/0.06      | 0.35/0.06      |
| Nitrogen concentration in fine roots live/dead          | %                    | 1.17/0.97   | 1.07/0.88      | 0.96/0.79      |
| Shading by maximum foliage                              | % of full light      | 8   | 16             | 30             |
| Soil volume occupied at maximum fine root biomass       | %                    | 100   | 98             | 95             |
| Efficiency of N root capture                            | %                    | 98  | 100            | 100            |
| Retention time for young/old foliage/dead branches      | years                | 1/2/40  | 1/2/40         | 1/2/40         |
| <b><i>Decomposition rates</i></b>                       |                      |   |                |                |
| Sapwood (by litter age)                                 | % year <sup>-1</sup> | 1-5 years (2.0); 6-10 years (10.0); 11-15 years (30.0); 16-20 years (20.0); >20 years (4.0)   |                |                |
| Heartwood   | % year <sup>-1</sup> | 1-10 years (0.4); 11-15 years (10.0); 16-24 years (15.0); 25-40 years (10.0); >40 years (2.0) |                |                |
| Bark  | % year <sup>-1</sup> | 1-5 years (2.0); 6-19 years (12.0); 20-40 years (20.0); >40 years (4.0)                       |                |                |
| Branches and large roots                                | % year <sup>-1</sup> | 1-5 years (10.0); 6-10 years (45.0); 11-15 years (35.0); >15 years (4.0)                      |                |                |
| Needles   | % year <sup>-1</sup> | 1-2 years (20.0); 3-5 years (30.0); 6-10 years (40.0); >10 years (2.0)                        |                |                |
| Fine roots  | % year <sup>-1</sup> | 1-2 years (30.0); 3-4 years (50.0); >4 years (9.0)  |                |                |



Table S3. FORECAST calibration parameters related to the simulation of litter decomposition and nutrient cycling for understory plants. Mineral soil parameters associated with nutrient storage are also shown (after Wei and Blanco, 2014).

| Parameter   | Unit                                     | Rich site   | Medium site     | Poor site    |
|---|--|---|-----------------|--------------|
| <b><i>Grass complex parameters</i></b>            |  |   |                 |              |
| Nitrogen concentration in stem live/dead          | %  | 1.65/0.30   | 1.38/0.25       | 1.10/0.20    |
| Nitrogen concentration in foliage live/dead       | %  | 2.04/1.67   | 1.70/1.30       | 1.36/0.93    |
| Nitrogen concentration in rhizome live/dead       | %  | 1.88/1.50   | 1.56/1.25       | 1.25/1.00    |
| Nitrogen concentration in roots live/dead         | %  | 0.08/0.06   | 0.06/0.05       | 0.05/0.04    |
| Shading by maximum foliage                        | % of full light                          | 5   | 15              | 25           |
| Soil volume occupied at maximum fine root biomass | %  | 60  | 55              | 50           |
| Efficiency of N root capture                      | %  | 99  | 99              | 99           |
| Retention time for foliage                        | years                                    | 1   | 1               | 1            |
| <b><i>Decomposition rates of grass</i></b>        |  |   |                 |              |
| Foliage   | % year <sup>-1</sup>                     | 99  |                 |              |
| Stems & roots (Poor site)                         | % year <sup>-1</sup>                     | 1 year (20.0); 2-4 years (30.0); 5-10 years (60.0); >10 years (2.0) |                 |              |
| Stems & roots (Medium site)                       | % year <sup>-1</sup>                     | 1 year (25.0); 2-4 years (35.0); 5-10 years (60.0); >10 years (2.0) |                 |              |
| Stems & roots (Good site)                         | % year <sup>-1</sup>                     | 1 year (30.0); 2-4 years (40.0); 5-10 years (60.0); >10 years (2.0) |                 |              |
| <b><i>Shrub complex parameters</i></b>            |  |   |                 |              |
| Nitrogen concentration in stem live/dead          | %  | 0.48/0.14   | 0.40/0.12       | 0.32/0.10    |
| Nitrogen concentration in foliage live/dead       | %  | 1.68/1.38   | 1.40/1.07       | 1.12/0.76    |
| Nitrogen concentration in rhizome live/dead       | %  | 1.14/1.05   | 0.95/0.86       | 0.76/0.70    |
| Nitrogen concentration in roots live/dead         | %  | 0.11/0.08   | 0.09/0.07       | 0.07/0.06    |
| Shading by maximum foliage                        | % of full light                          | 20  | 30              | 45           |
| Soil volume occupied at maximum fine root biomass | %  | 60  | 55              | 50           |
| Efficiency of N root capture                      | %  | 99  | 99              | 99           |
| Retention time for foliage                        | years                                    | 1   | 1               | 1            |
| <b><i>Decomposition rates of shrub</i></b>        |  |   |                 |              |
| Foliage (poor site)                               | % year <sup>-1</sup>                     | 1 year (80.0); 2-3 years (60.0); 4-5 years (50.0); >5 years (2.0)   |                 |              |
| Foliage (Medium site)                             | % year <sup>-1</sup>                     | 1 year (90.0); 2-3 years (60.0); 4-5 years (50.0); >5 years (2.0)   |                 |              |
| Foliage (Good site)                               | % year <sup>-1</sup>                     | 1 year (95.0); 2-3 years (60.0); 4-5 years (50.0); >5 years (2.0)   |                 |              |
| Stems & roots (poor site)                         | % year <sup>-1</sup>                     | 1 year (20.0); 2-3 years (30.0); 4-5 years (40.0); >5 years (2.0)   |                 |              |
| Stems & roots (Medium site)                       | % year <sup>-1</sup>                     | 1 year (25.0); 2-3 years (35.0); 4-5 years (40.0); >5 years (2.0)   |                 |              |
| Stems & roots (Good site)                         | % year <sup>-1</sup>                     | 1 year (30.0); 2-3 years (40.0); 4-5 years (40.0); >5 years (2.0)   |                 |              |
| <b><i>Soil parameters</i></b>                     |  |   |                 |              |
| Nitrogen concentration in slow/fast humus         | %  | 3.00/1.40   | 3.00/1.40       | 3.00/1.40    |
| Decomposition rate slow/fast humus                | % year <sup>-1</sup>                     | 0.15/2.00   | 0.15/2.00       | 0.15/2.00    |
| CEC soil (CEC humus)/AEC                          | kg N ha <sup>-1</sup>                    | 80.0 (0.2)/20.0   | 60.0 (0.2)/10.0 | 40 (0.2)/5.0 |
| Atmospheric deposition/non-symbiotic fixation     | kg N ha <sup>-1</sup> year <sup>-1</sup> | 4.9/1.0   | 4.9/1.0         | 4.9/1.0      |

## 2 Simulating the Effect of Increasing CO<sub>2</sub> on Future Water Stress

Recent literature reviews have reported increases in tree water use efficiency (WUE) associated with increasing atmospheric CO<sub>2</sub> concentrations ( $c_a$ ) (e.g. Battipaglia et al., 2013; Silva and Anand, 2013). Whether artificially induced or associated with long-term trends, increases in  $c_a$  have generally led to decreases in stomatal conductance of water vapour and increases in tree WUE (Ainsworth and Rorgers, 2007; Keenan et al., 2013). ForWaDy was developed to simulate the impact of forest management on stand-level hydrological processes, and the initial version did not allow for a representation of the effect of increasing atmospheric CO<sub>2</sub> concentrations on stomatal conductance and WUE.

The original version of ForWaDy has been modified to facilitate its application for climate change analysis including different CO<sub>2</sub> emissions scenarios. This was achieved through the use of a function to adjust the species-specific canopy resistance term ( $R_{Can,i}$ ) based on historical trends and projected changes in  $c_a$ . The function was developed to represent the relationship between relative stomatal conductance for water vapour ( $g_{w(rel)}$ ) and  $c_a$  identified through a meta-analysis conducted by Franks et al. (2013; Fig. S1A). The functional curve is derived from the physiological relationship between relative net assimilation rate  $A_{n(rel)}$  and changes in  $c_a$  relative to a reference atmospheric CO<sub>2</sub> concentration ( $c_{a0}$ ) as described in Equation S1. The effect of changes in  $c_a$  can be related in terms of  $g_{w(rel)}$  according to Equation S2 (Franks et al., 2013). Finally, expected changes in  $g_{w(rel)}$  are used to estimate changes in canopy resistance ( $R_{Can,adj}$ ) associated with specific future CO<sub>2</sub> emission scenarios (Eq. S3) in ForWaDy. An example of the effect of increasing  $c_a$  on  $R_{Can,adj}$  is shown for Chinese fir with an  $R_{Can}$  value of 0.3 (Fig. S1B).

$$A_{n(\text{rel})} = [(c_a - r^*) * (c_{a0} + 2r^*)] / [(c_a + 2r^*) * (c_{a0} - r^*)] \quad (\text{S1})$$

where:

$A_{n(\text{rel})}$  = relative net assimilation rate

$c_a$  = current atmospheric CO2 conc (ppm)

$c_{a0}$  = reference atmospheric CO2 conc (determined from reference climate data, ppm)

$r^*$  = CO2 compensation point = 40 ppm

$$g_{w(\text{rel})} = A_{n(\text{rel})} / c_{a(\text{rel})} \quad (\text{S2})$$

where:

$g_{w(\text{rel})}$  = relative stomatal conductance for water vapour (dimensionless)

$c_{a(\text{rel})}$  = relative atmospheric CO2 conc =  $c_a / c_{a0}$  (dimensionless)

$$R_{\text{Can,adj}} = R_{\text{Can}} + R_{\text{Can}} * (1 - g_{w(\text{rel})}) \quad (\text{S3})$$

where:

$R_{\text{Can,adj}}$  = adjusted canopy resistance (dimensionless)

$R_{\text{Can}}$  = reference canopy resistance (dimensionless)

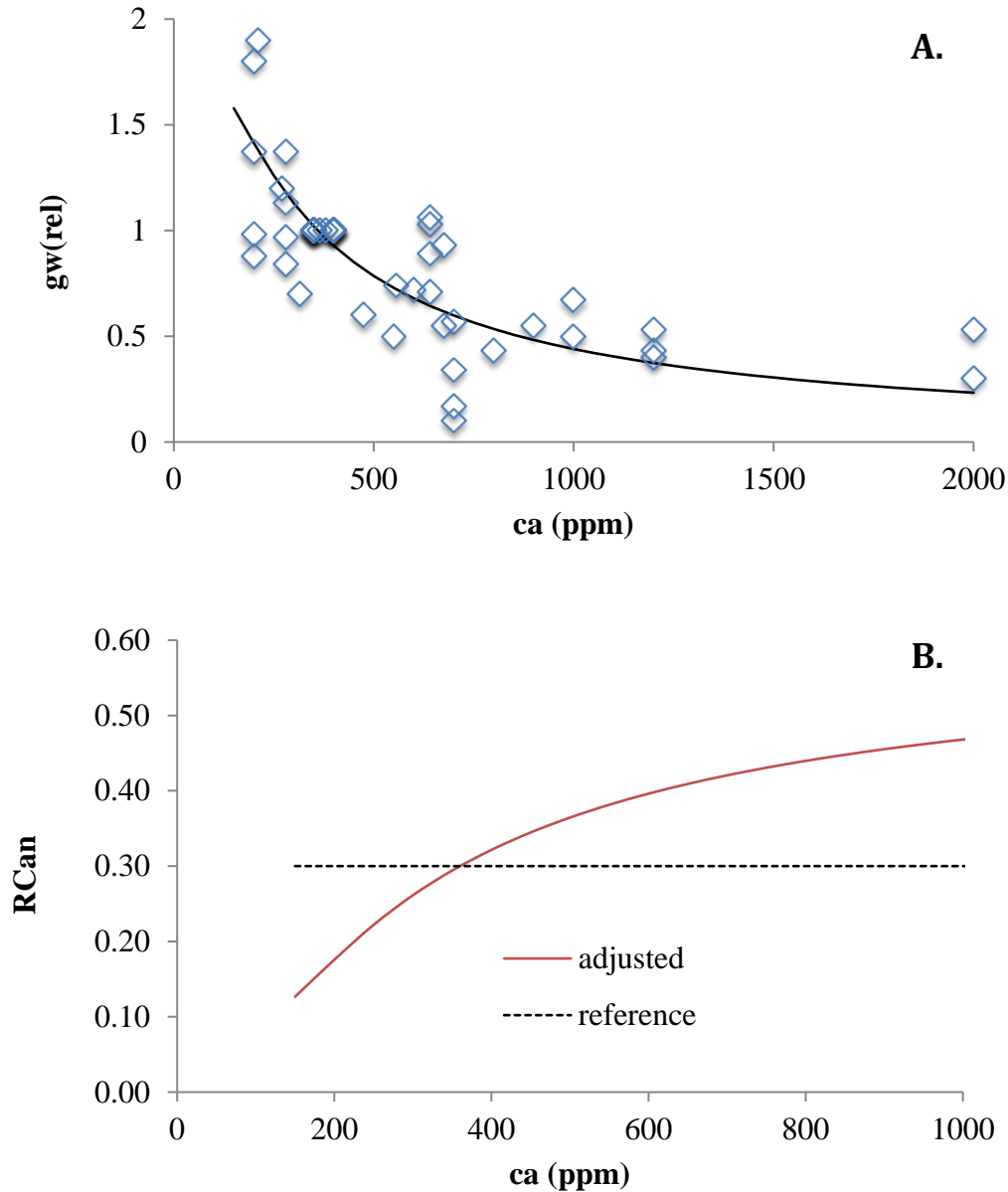


Figure S1. A) Observations of relative stomatal conductance for water vapour ( $g_w(\text{rel})$ ) under changing atmospheric  $\text{CO}_2$  concentrations ( $c_a$ ; re-plotted from Franks et al., 2013) and B) an example of the calculation of adjusted canopy resistance ( $R_{Can,adj}$ ) as a function of  $c_a$  based upon Equation 3 for Chinese fir with a reference value of  $R_{Can}$  of 0.3.

### 3 Sensitivity Analysis

A two-part sensitivity analysis was conducted to evaluate the sensitivity of the model response to changes in atmospheric  $\text{CO}_2$  concentrations and to potential changes in growing-season rainfall patterns. The impact of changing  $\text{CO}_2$  concentrations was

assessed by running the climate change scenarios described in Section 2.5.2 without the corresponding changes in atmospheric CO<sub>2</sub> concentrations (atmospheric CO<sub>2</sub> was held at 396ppm). To evaluate the impact of changes in growing season rainfall patterns, a new set of climate change scenarios were generated in which the frequency of growing season (Mar - Oct) precipitation events were reduced by 35% while maintaining the total monthly rainfall amounts. The scenarios were created using the Statistical Downscaling Model (SDSM v5.2) developed by Wilby and Dawson, 2013. These were intended to represent potential increases in rainfall intensity associated with climate warming.

Results from the sensitivity analysis show that the calculation of water stress in the model is sensitive to both changes in atmospheric CO<sub>2</sub> concentration and the frequency and intensity of growing season precipitation events (Table S4). Removing the effect of CO<sub>2</sub> on water use efficiency (by holding CO<sub>2</sub> constant) led to average increase of water stress of 22% above the levels observed for the original scenarios. Similarly, decreases in the frequency of growing season precipitation events led to an average increase of 24% in the mean annual water stress index (TDI) relative to the original scenarios. However, despite the increase in water stress, biomass production at rotation only declined slightly (1 to 2%) in the sensitivity analysis runs (Table S5). The impact of the increased water stress was small because although it increased, water stress was still low enough that it had only a minimal impact on growth and mortality.



Table S4. Sensitivity analysis results showing the relative impact of the inclusion of the effects of changes in atmospheric CO<sub>2</sub> concentrations and growing season (Mar-Oct) precipitation patterns on modelled water stress index organized by rotation climate change scenario. The columns represent different the parameter settings (see footnotes for detail). The numbers represent the relative change (+ = increase; - = decrease) from the reference climate run.

| <b>HG 4.5</b>                   |           |       |       |       |       |
|---------------------------------|-----------|-------|-------|-------|-------|
|                                 | Rotation  | P0_A0 | P0_A1 | P1_A0 | P1_A1 |
| Change from<br>reference<br>(%) | <b>R1</b> | -22%  | -17%  | 7%    | 12%   |
|                                 | <b>R2</b> | -19%  | -4%   | 19%   | 39%   |
|                                 | <b>R3</b> | -2%   | 26%   | 33%   | 59%   |
| <b>HG 8.5</b>                   |           |       |       |       |       |
| Change from<br>reference<br>(%) | <b>R1</b> | -10%  | -4%   | 17%   | 24%   |
|                                 | <b>R2</b> | -16%  | 12%   | 9%    | 41%   |
|                                 | <b>R3</b> | 2%    | 55%   | 33%   | 86%   |
| <b>CNRM 4.5</b>                 |           |       |       |       |       |
| Change from<br>reference<br>(%) | <b>R1</b> | -10%  | -5%   | 0%    | 7%    |
|                                 | <b>R2</b> | -8%   | 12%   | 0%    | 16%   |
|                                 | <b>R3</b> | 12%   | 35%   | 38%   | 73%   |
| <b>CNRM 8.5</b>                 |           |       |       |       |       |
| Change from<br>reference<br>(%) | <b>R1</b> | 3%    | 12%   | 32%   | 42%   |
|                                 | <b>R2</b> | 10%   | 46%   | 25%   | 60%   |
|                                 | <b>R3</b> | 43%   | 122%  | 57%   | 132%  |
| <b>Average</b>                  |           |       |       |       |       |
| Change from<br>reference<br>(%) | <b>R1</b> | -10%  | -4%   | 14%   | 21%   |
|                                 | <b>R2</b> | -8%   | 16%   | 13%   | 39%   |
|                                 | <b>R3</b> | 14%   | 59%   | 40%   | 88%   |

P0 = Original precipitation

P1 = 35% fewer rainfall events during growing season

A0 = including effect of increasing CO<sub>2</sub> on WUE

A1 = no effect of increasing CO<sub>2</sub> on WUE

Table S5. Sensitivity analysis results showing the relative impact of the inclusion of the effects of changes in atmospheric CO<sub>2</sub> concentrations and growing season (Mar-Oct)

precipitation patterns on stemwood biomass production organized by rotation climate change scenario. The columns represent different the parameter settings (see footnotes for detail). The numbers represent the relative change (+ = increase; - = decrease) from the reference climate run.

| <b>HG 4.5</b>             |           |              |              |              |              |
|---------------------------|-----------|--------------|--------------|--------------|--------------|
|                           | Rotation  | <b>P0_A0</b> | <b>P0_A1</b> | <b>P1_A0</b> | <b>P1_A1</b> |
| Change from reference (%) | <b>R1</b> | 6.6          | 6.7          | 8.5          | 8.6          |
|                           | <b>R2</b> | 10.3         | 9.3          | 8.7          | 10.9         |
|                           | <b>R3</b> | 11.5         | 11.8         | 11.6         | 10.7         |
| <b>HG 8.5</b>             |           |              |              |              |              |
| Change from reference (%) | <b>R1</b> | 8.1          | 7.6          | 9.8          | 8.7          |
|                           | <b>R2</b> | 12.1         | 14.3         | 10.8         | 13.7         |
|                           | <b>R3</b> | 17.1         | 16.1         | 16.7         | 15.5         |
| <b>CNRM 4.5</b>           |           |              |              |              |              |
| Change from reference (%) | <b>R1</b> | 5.4          | 3.9          | 6.0          | 6.8          |
|                           | <b>R2</b> | 6.1          | 6.3          | 5.8          | 4.7          |
|                           | <b>R3</b> | 4.5          | 4.4          | 4.3          | 5.4          |
| <b>CNRM 8.5</b>           |           |              |              |              |              |
| Change from reference (%) | <b>R1</b> | 6.0          | 6.1          | 6.2          | 6.6          |
|                           | <b>R2</b> | 9.5          | 9.3          | 10.4         | 9.8          |
|                           | <b>R3</b> | 13.8         | 13.3         | 11.9         | 11.9         |
| <b>Average</b>            |           |              |              |              |              |
| Change from reference (%) | <b>R1</b> | 6.5          | 6.1          | 7.6          | 7.7          |
|                           | <b>R2</b> | 9.5          | 9.8          | 8.9          | 9.8          |
|                           | <b>R3</b> | 11.7         | 11.4         | 11.1         | 10.9         |

P0 = Original precipitation;

P1 = 35% fewer rainfall events during growing season but retain amounts;

A0 = increasing atm CO<sub>2</sub>;

A1 = constant CO<sub>2</sub> (396ppm).

## References

- Ainsworth, E. A. and Rogers, A. The response of photosynthesis and stomatal conductance to rising [CO<sub>2</sub>]: mechanisms and environmental interactions. *Plant Cell Environ* 2007; 30: 258–270.
- Battipaglia, G. , M. Saurer, P. Cherubini, C. Calfapietra, H. R. McCarthy, R. J. Norby, and M. F. Cotrufo. Elevated CO<sub>2</sub> increases tree-level intrinsic water use efficiency: insights from carbon and oxygen isotope analyses in tree rings across three forest FACE sites. *New Phytol* 2013; 197: 544–554.
- Franks, P.J., Adams, M.A., Amthor, J.S., Barbour, M.M., Berry, J.A., Ellsworth, D.S., Farquhar, G.D., Ghannoum, O., Lloyd, J., McDowell, N., Norby, R.J., Tissue, D.T., von Caemmerer, S. Sensitivity of plants to changing atmospheric CO<sub>2</sub> concentration: from the geological past to the next century. *New Phytol* 2013; 197: 1077-1094.
- Keenan, T. F., D. Y. Hollinger, G. Bohrer, D. Dragoni, J. W. Munger, H. P. Schmid & A. D. Richardson. Increase in forest water-use efficiency as atmospheric carbon dioxide concentrations rise. *Nature* 2013; 499: 324-327
- Silva, L. C. R. and M. Anand. Probing for the influence of atmospheric CO<sub>2</sub> and climate change on forest ecosystems across biomes. *Global Ecology Biogeography* 2013; 22: 83–92.
- Wei X, Blanco JA. Significant increase in ecosystem C can be achieved with sustainable forest management in subtropical plantation forests. *PLoS ONE* 2014; 9: e89688.
- Wilby, R.L.; Dawson, C.W. The statistical downscaling model: insights from one decade of application. *Int. J. Climatol.* 2013, 33, 1707-1719.
- Xin Z, Jiang H, Jie C, Wei X, Juan B, Zhou G. Simulated nitrogen dynamics for a *Cunninghamia lanceolata* plantation with selected rotation ages. *Journal of Zhejiang A&F University* 2011; 28: 855-862. [In Chinese].